International Journal of Mechanical and Production Engineering Research and Development (IJMPERD)
ISSN(P): 2249-6890; ISSN(E): 2249-8001
Vol. 9, Issue 3, Jun 2019, 1749-1760

THE GRAPHIC ANALYTICAL METHOD OF FLAT SOLAR COLLECTOR ENERGETIC AND OPTICAL CHARACTERISTICS

YE. N. AMIRGALIYEV[1,2], M. KUNELBAYEV[1,2], T. MEREMBAYEV[1], S. DAULBAYEV[1] & A. IRZHANOVA[1]

[1]*Institute Information and Computational Technologies CS MES RK, Kazakhstan*

[2]*Al-Farabi Kazakh National University, Kazakhstan*

ABSTRACT

The work herein considers the graphic-analytical method of the flat solar collector's energetic and optical characteristics. There has been computed the total solar radiation on the solar collectors' inclined surfaces. In the research methodology, as an example of the total solar radiation computation, there has been taken Astana city. According to the observation data it is seen, that the solar radiation duration falls in summer. So, by means of graphic-analytical method there has been computed the distributions of direct solar radiation flow stream density, optical performance coefficient from direct solar radiation flow stream density and total flow to the receiver. Optical performance coefficient has constituted 66%.It proves the correctness of the solar collector parameters selection.

KEYWORDS: Sun, Radiation, Graphic Analytical Method & Optical Performance Coefficient

Received: Apr 03, 2019; **Accepted:** Apr 23, 2019; **Published:** Jun 14, 2019; **Paper Id.:** IJMPERDJUN2019187

Original Article

INTRODUCTION

Scope of technogenic impact on the environment and sustainable demand for the power underlines the urgent transfer to the renewable energy sources. Solar thermal collectors market is 8 times bigger, than it has been twenty years ago, as the solar collector is more efficient, than a photovoltaic system for heat production [1]. Apart from that, the cheaper storage, comparable with accumulators, has made the solar thermal collectors more profitable for the heat production, than photovoltaic systems. The solar thermal collectors are usually broken down into three categories based on the heat transfer fluid (HTF) temperature. Low temperature solar collector (less than 100°C) consists of a flat plate and evacuated tube collectors (ETC), which are able to maintain the hot water and air for residential properties, high temperature collector (over 300°C) [2,3]. Such linear Fresnel collectors and parabolic ducts, are, by and large, designed for the steam generators vapor provision [4]. Finally, the less studied category represents an average temperature collector (100-300°C) with a wide spectrum application, for instance, desaltation [5], mining operations, vapor generation [6] and zero liquid [7].

Various approaches to an optical analysis have been carried out by several researches. Jose has analyzed the flow distribution in the solar furnace focal spot considering the sun limb darkening [8]. Evans has used an integral dependence to determine the intensity both of flat absorbers and, cylindric and parabolic concentrators under perfect conditions, supposing the sun disc [9]. Dali has made use of the back-beam tracking procedure to define the flow distribution according to the solar concentrator [10]. Nicolya has conducted a flow distribution

two-dimensional analysis at parabolic collectors and included the influence of the incidence angle at the flow distribution for flat surfaces [11]. Jeter has studied the intensity distribution around the circular receivers, using the semi-infinite formula, considering the sun as a point source. As well, he has investigated the declination influence at the flow distribution. Jeter has worked out a semi-infinite model for computing the flow distribution, considering a glass tube effects through including transmission and absorption functions [12]. Kaushik developed the main optics analytical models for paraboloid concentrators and analyzed the experimental concentrators operation [13]. Calogiro has used the artificial neuron networks for defining the flow distribution in the cylindrical absorber for different solar energy inclination angles [14]. Gombert et al. worked on the surfaces with antiglare covers with long waves and informed about transmission increases comparing the existing antiglare plating [15]. Eck and Steinmann have elaborated an analytical model for vapor direct production. There has been presented the correlation for the mass minimal flow to avoid a stratified stream. As well, there has been discussed the minimal temperature at the collector input to evade the stress instability [16].

Grena, by means of optical method, has simulated the parabolic duct collector, applying the Monte Carlo simulation method, accounting tracing mistakes, incidence angle and diffraction in the glass tube [17]. Yang et al. have analyzed the flow distribution in the parabolic duct collector by means of Monte Carlo method [18]. Kumar and Raddy have applied an analytical method to determine the intensity distribution on the flat receivers. The surface mistakes affect is included into a scattering angle. Dispersion mistake is computed along the image width by analytical approach technique [19]. Y.L. Heet al. has integrated the Monte Carlo modeling with a finite volume method to obtain the receiver walls temperature gradient. To compute the flow intensity there have been accepted the uniform values of the glass tube transmission and receiver's absorptive ability [20]. Cooper and Steinfeld have described the mirror mistakes at reflecting surfaces. Angular dispersion azimuth error is considered to be defined and analytically obtained and equals to the known Rayleigh distribution through two-dimensional circular distribution in polar coordinates [21]. Francini et al. have elaborated the methodology for measuring the slopes defects by means of reflected image on the receiver [22]. Wirz et al. have developed the bounded method MCRT with finite elements solver for getting the temperature distribution along the absorber cross-section for the collectors on the oily base [23]. Cheng et al. have studied the sensitivity of industrial parabolic duct collector's different configurations in regard to the tracking errors. There has been made a conclusion, that a flatter is more sensitive to a surface error, than error tracking. There has been revealed a surface and tracking errors threshold value [24].

In the article herein the researches consider a graphic-analytical method of identifying the flat solar collector's power and optical characteristics. To research the graphic-analytical method the developers have investigated a new flat solar, as well, carried out experimental researches of energetic and optical characteristics.

METHOD OF RESEARCH

Graphic-analytical method of determining the concentrating systems energetic characteristics is based on the geometrical constructions, which allow defining the displaying on the receiver of rays beam, reflected by a mirror elementary area [25]. At that, there is used a mirror reflection rule and considered either a parallel rays beam or a divergent one with an angular dimension $\varphi_0 \geq \varphi_C$. Radiation distribution in the beam per directions is accepted to be uniform, and, at the necessity of distribution non uniformity account, a reflected beam is broken down into a number of elementary beams with uniform distribution. Mirror global geometry is usually assigned in the form of the certain configuration perfect mathematical surface. Analysis of obtained, upon the beam distribution tracking, geometrical figures gives a possibility to

express the sizes of the mirror elementary area and the beam reflection on the receiver through the same concentrating system's specific parameters and to find their ratio, determining the elementary geometrical concentration factor. Integrating the latter along the complete reflecting surface allows specifying the average or local value of the factor thereof on the receiver.

The method thereof is rather labor consuming and, at large, already does not correspond to the modern calculation practice, focused at using the computations by means of computer programs. But in some cases, for instance, upon computing the systems with flat reflectors in single beam approximation, it allows quickly enough obtain the dependence between concentration coefficient and system's elements reference sizes, therefore it might be recommended for practical use. However, the graphic-analytical method's main advantage, not still losing its applicability, is linked with the possibility of clearly evident qualitative analysis of radiant flux distribution in the system, which is always useful at the investigation initial stage.

The concentrating system basic energetic feature is an average concentration coefficient K_C, which is defined as the ratio of the average value of concentrated radiant flux density on the receiver E_{ecp} to the solar radiation surface density in the plane, perpendicular to its distribution direction E_C, or to the round lenses (our concentrator is their analog) with a square of F_1 and circular receivers with F_2 square will be equal to duplicate ratio of their radii.

To assess the potential of solar energy, falling on the territory in any region it is necessary to have the data on the solar energy potential. Being based on the real observations and theoretical computations generalization, we confirm, that there exist the annual and lateral movement of possible monthly and annual sums of direct solar radiation, falling onto the perpendicular surface under clear sky conditions, data on sunshine period, sun light daily movement, radiation during standard yearly days, maps of monthly average radiation sums distribution for June and December on Kazakhstan territory [26].

Total irradiation yearly amounts constitute, in tropical and subtropical latitudes, over 140 kcal /cm2. They are particularly big in mainly clear subtropical deserts, and in the Northern Africa reach 200-220 kcal/cm2. Buy over subequatorial forest areas with their high clouded sky (over Amazonia and Kongo basins, over Indonesia) they are lowered down to 100-120 kcal/cm2. Towards higher latitudes of both hemispheres the total radiation amounts decrease, constituting about 60° latitude to 60-80 kcal/cm2. But further they grow again – a little in the northern hemisphere, but rather sufficiently over clear sky and snowy Antarctic Continent, where in the continent depth they reach 120-130 kcal/cm2, i.e., the values, close to tropical and exceeding equatorial. Over the oceans the radiation total is lower, than over the land [27].

In December the highest total radiation is up to 20-22 kcal/cm2 and even higher in the southern hemisphere deserts. But in cloudy regions at the equator they are decreased down to 8-12 kcal/cm2. In winter northern hemisphere the irradiation is quickly decreased toward the North; to the North the 50th parallel it is less than 2 kcal/cm2 and a little towards the north polar circle it equals to zero. In summer southern hemisphere it descends to the south down to 10 kcal/cm2 and lower in the latitudes 50-60°. But further it increases up to 20 kcal/cm2 at Antarctica shores and it exceeds 30 kcal/cm2 inside Antarctica, where it is, thus, higher, than in summer in tropics [27].

There is the highest radiation, over 22 kcal/cm2, over north-east Africa, Arabia, Plateau of Iran. It is up to 20 kcal/cm2 and higher in Central Asia; sufficiently less, down to 14 kcal/cm2, in tropical parts of the southern hemisphere continents. In cloudy subequatorial areas it, as in December, decreases down to 8-12 kcal/cm2. In summer northern

hemisphere the radiation becomes less from subtropics to the north slowly, and to the north of 50° northern latitude it increases, reaching 20 kcal/cm2 and more in the Arctic basin. In winter southern hemisphere the radiation reduces to the southern direction, down to zero after the southern polar circle [27].

As an example of using the solar irradiation there has been taken Astana city, capital of Kazakhstan. As we can see from the figure 4 – sunshine period and number of days, Astana city is located higher, than Kazakhstan's southern regions, and has a certain potential for the solar energy development within the period from April to October (Figure.1). Number of sunny hours reaches 2200 hours per a year [28].

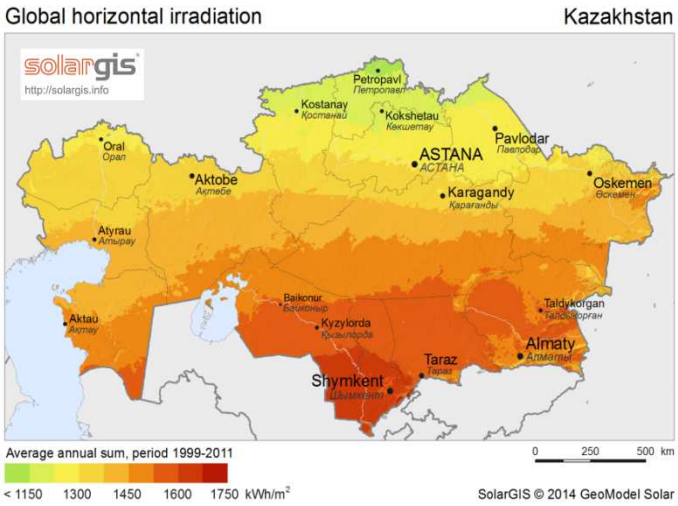

Figure 1: Kazakhstan Solar Irradiation Map. (National atlas of the Republic of Kazakhstan, 2006)

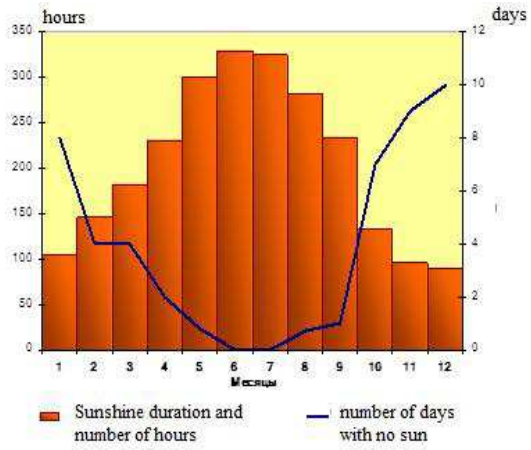

Figure 2: Sunshine Duration and Number of Days without Sun in Astana

The Figures 1 and 2 show the map of the solar radiation in Kazakhstan and number of days without sun in Astana. Proceeding from the results of the average values of direct, total radiation and duration of sunlight statistical processing there have been differentiated five zones and drawn up a histogram, characterizing the sunshine period in Astana.

RESULTS OF RESEARCH

In the research of the solar collectors with reflectors and transparent insulation made of vacuumed glass envelopes there is provided the computation of mentioned solar collectors' energetic and optical specifications, including graphic-analytical method of the solar collector optical efficiency factor computing. The solar collectors' reflectors have been

designed so as the reflected rays fall on the thermal receiver's backside. To maintain the balanced condition the computation of the solar collector's (with reflectors) thermal balance is carried out according to the equation [29]:

$$H\tau\eta_{onm}\Theta = q_{пр.из} + q_{мепл.из} \quad (1)$$

where H-total solar radiation density, Wt/m^2, τ- transparent insulation transmission coefficient; η_{onm}- systems' optical efficiency factor; Θ-solar irradiation wash-out rate; $q_{пр.из} - density\ of\ the\ thermal\ flow\ through\ transparent\ insulation$, Wt/m^2; $q_{мепл.из}$-density of the thermal flow through thermal insulation, Wt/m^2.

System's optical efficiency factor η_{onm} is assumed to be computed by means of graphic analytical method, lying in dividing the solar flow, falling onto the solar collector (normal falling), into the zones according to reflections number from the solar collector.

The total flow, falling on the receiver, will be formed with the direct flow, falling onto the receiver's face side, and with the flow, reflected from a concentrator to the receiver's backside (provided $r_{пр} \leq r \leq R_{an} u\ r_{пр} = r_0$) [29]:

$$Q = \alpha_{пр} q\pi[(r_n{}^2 - r_{n-1}{}^2)\rho^n + (r_{n-1}{}^2 - r_{n-2}{}^2)\rho^{n-1} + (r_{n-2}{}^2 - r_{n-3}{}^2)\rho^{n-2} + \cdots$$
$$+(r_1{}^2 - r_0{}^2)\rho^1 + \delta_0 r_{пр}{}^2\rho^0] \quad (2)$$

where q – direct solar radiation flow density, Wt/m^{22}; $r_n = R_{an}$ – great circle concentrator's (aperture) radius; r_{n-1}– peripheral ring's inner radius and external radius of the ring following it; ρ_n – concentrator's reflection index in the degree n; $\alpha_{пр}$ – absorption coefficient of solar radiation by a receiver; r_0 – a radius to semi-circumference axis; $r_{пр}$ – receiver's radius; $\delta_0 \geq 1$ – the factor, accounting the scattered radiation, falling onto the receiver's face side.

The zone of arrays distribution according to reflections number in the flat solar collector is shown on the Figure 3 [30].

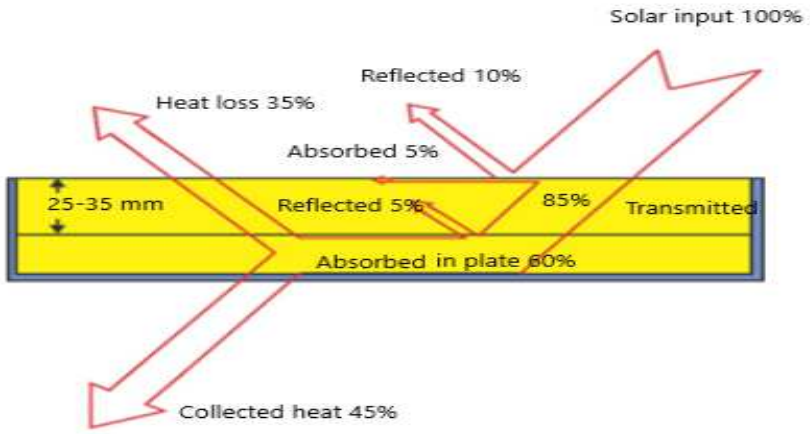

Figure 4: Influence of the Solar Irradiation at the Flat Solar Collector

In the collector the solar rays fall on the receiver's surface, which is heated and further transmits the thermal energy through the liquid absorber. In other words, the solar emission share, received by the heat carrier, totally depends on the absorber, which keeps the liquid from a direct contact with the sun light, as it is shown on the Figure 4.

For the solar collector with reflectors (Figure 3) the flow, incoming to the receiver, will equal to [29]:

$$Q = 2\alpha_{np} q L_k [(r_n - r_{n-1})\rho^n + (r_{n-1} - r_{n-2})\rho^{n-1} + (r_{n-2} - r_{n-3})\rho^{n-2} + \cdots + (r_1 - r_0\rho^1 + \delta r_{np}\rho^0)] \quad (3)$$

where L_k – concentrator's length, m; r_{np}, r_n herein is the receiver's width and the zone's width accordingly, m.

Optical coefficient factor η_{onm} of the system «concentrator – receiver» is defined as [29]

$$\eta_{onm} = \frac{Q}{\delta_0 q * A_{an}} \quad (4)$$

where A_{an} – reflector's aperture square.

For solar collector with reflectors η_{onm} = 66 % at ρ = 0,9.

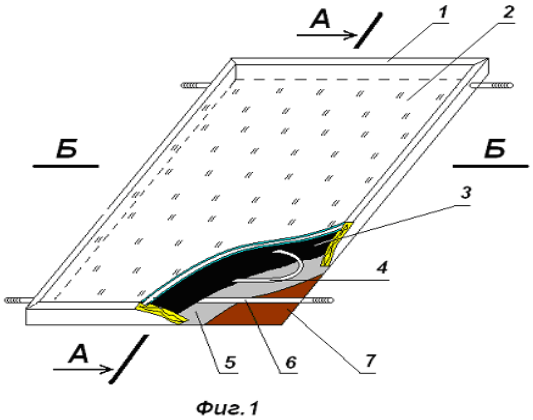

Figure 5: Solar Collector in Section

The Figure 5 demonstrates the flat solar collector's mock up. Contents and novelty consist in the fact, that in distinction from the known designing principle, the collector contains a transparent glass envelope 2 with double glass and reduced stress, as well as, a perimeter frame 1. Wood frame bottom 7 is made of 8 mm width plywood and stuck with a heat insulating film 5 with foil. In the gap, formed between a glass envelope and frame bottom there is laid a flexible thin-walled stainless corrugated tube 4∅16 mm in the coil form. Pipe edges are fixed to input and output protrusive tubes 6.

Figure 6: Flat Solar Collector Mock Up

Figure 6 presents the flat solar collector mock up. The solar collector is the main heat producing unit of the solar installation. To achieve the purpose in view, we have elaborated a principally new flat solar collector, on the base of which there will be created the solar collectors' standard series for water heating and heating of buildings and premises.

Table 1: Technical Specifications of Flat Plate Solar Collector

Parameters	Value
Adsorbent plate material	Copper
Adsorbent plate size	1000×2000 mm^2
Adsorbent plate width	0.4 mm
Glazing material	Red hot glass
Glazing sizes	1000×2000 mm^2
Glazing width	4 мм
Insulation	Foam plex (foamed polyurethane)
Collector's slope angle	45^0
Absorber's thermal conductivity	401 W/(m K)
Insulation thermal conductivity	0.04 W/(m K)
Transmission-absorption factor	0.855
Apparent sun temperature	4350 K
Environmental temperature	303 K
Radiation rate	1000 W/m^2

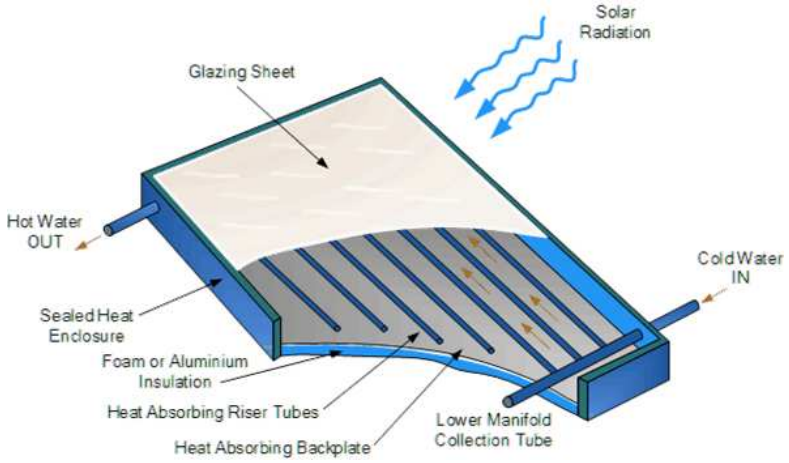

Figure 7: Penetration of Solar Irradiation into the Flat Solar Collector

Figure 7 shows that absorbed solar radiation reaches the collector's interiority, either passing through the wall to the wall's internal surface, to which it is directed and reflected from, or with a hot air, going through an air gap. The wall loses the energy for the environment due to conductivity, convection and reflection through the glazing. Upon penetrating the solar irradiation into the flat solar collector due to additional solar heat accumulation on the absorber surface, the change in speed of the working liquid stream is inevitable. Consequently, an absorber material proper selection and working liquid play an important role in the thermal flow collection.

From the Table 2 it is seen, that at heat carrier equal consumption (water) the maximum temperature is reached in the solar collector with reflectors and transparent insulation and constitutes 94°C. Such temperature is high enough at concentration coefficient 2. Solar collector's (with reflectors) efficient factor amounts to 40,1 %, which is for 10,8 % higher, than that of the solar collector with reflectors and single layer glazing.

Table 2: Parameters of Environment and Solar Collector with Various Glazing Types at Heat Carrier Maximum Heating

Glazing type	o t_{oc}, C	H, Wt/m^2	$Hnpux$, Wt·h/m^2	T_{input}, oC	T_{output}, oC	T_{output}– T_{input}, °C	G, kg/h·m^2	Q, Wt·h/m^2	η, %
One glass	20,5	715	732,7	22	78	56	3,3	214,4	29,3
Double glazing, gap 3 mm	17	722	739,9	19	82	63	3,4	248,5	33,6

Symbols in the Table: t_{oc} – environment temperature, H – solar irradiation; H_{npux}– solar irradiation amount per hour; $t_{вх}$– heat carrier temperature (water)at the solar collector input, $t_{вых}$ – heat carrier temperature at the solar collector output; G – heat carrier consumption, Q – thermal energy, obtained in the collector during an hour; η – efficient factor.

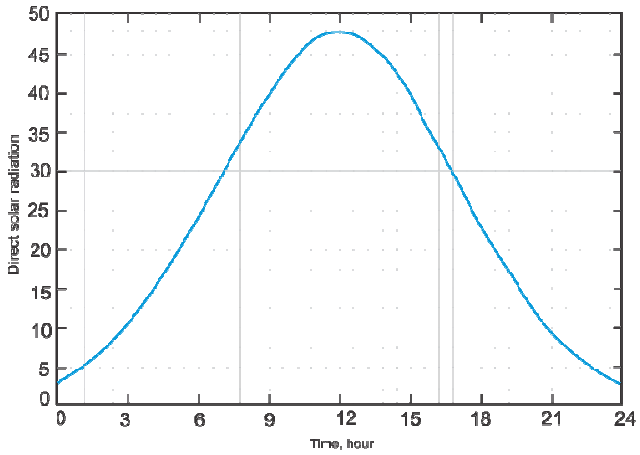

Figure 8: Graph of Distributing Direct Solar Irradiation Flow Density, Wt./m2 for 24 hours

The Figure 8 shows, that within a day, that is 24 hours the direct solar irradiation flow density is effective in the middle of the day, in other words, when the sun is in the zenith of its location. As well, the dependence shows, that the higher the direct solar radiation flow density, the higher the air temperature.

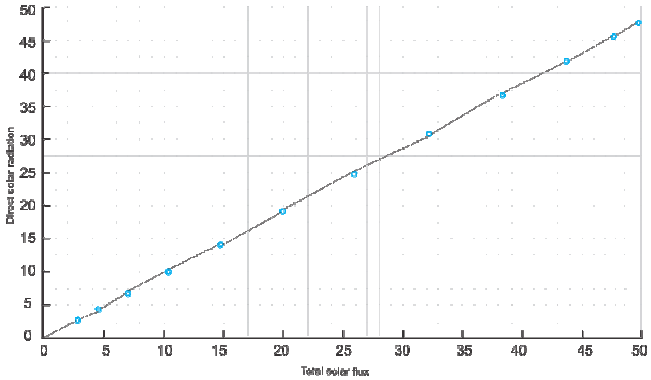

Figure 9: Graph of Optical Performance Factor Dependence on Direct Solar Radiation Flow Density and Total Flow to the Receiver

From the Figure 9 it is seen, that the higher the solar collector's optical efficient factor, the higher the flow density and the total flow to the receiver. As well, the higher the total flow to the receiver, the higher the solar collector's optical efficient factor.

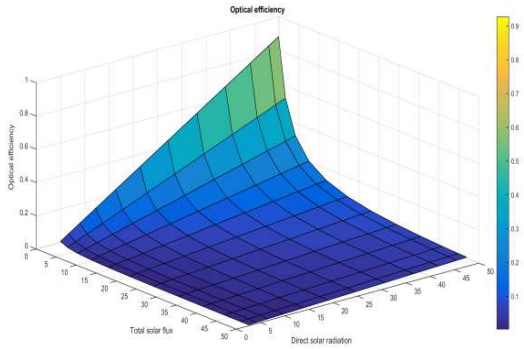

Figure 10: Dependence of Direct Solar Radiation Flow Density on Total Flow to Receiver

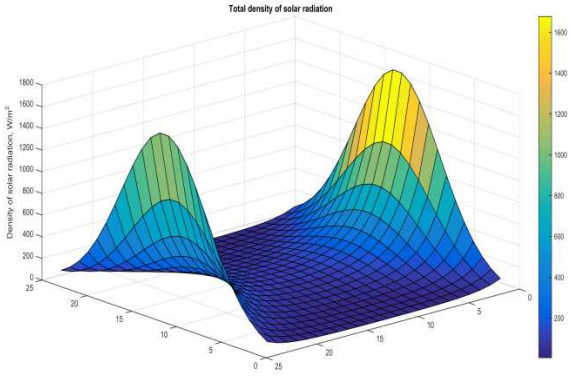

Figure 11: Values of Total Solar Radiation Density, Obtained from the Equation for Balanced Condition Solar Collector with the Deflectors

Solar radiation falling onto the horizontal surface at clear sky in midday hours on the territory's horizontal part constitutes 0.33-0.81 kWt/m^2, in mountainous regions – 0.46-1.02 kWt/m^2. Cloud cover decreases incoming solar radiation and radiation balance.

The total radiation is defined with a total fall of direct and scattered radiation on the horizontal surface. Total radiation maximum intensity is reached in May-July on the whole territory of the republic. Total radiation intensity changes in submontane regions from 280 to 925 mJ/m2. In high mountain areas it fluctuates from 360 to 1120 mJ/m2

CONCLUSIONS

The work herein presents the graphic-analytical method for defining the energetic and optical specifications of the flat solar collector. There have been obtained the direct solar radiation flow density distributions during 24 hours in Astana city per a day, that is, the dependence shows, that the higher the direct solar radiation flow density, the higher the air temperature. Also, there is obtained the dependence of optical efficient factor on the direct solar radiation flow density and total stream to the receiver. As well, the higher the total flow to the receiver, the higher the solar collector's optical efficient factor. In the course of experimental researches it was revealed, that defining by means of graphic-analytical method the solar collector's thermal features, with different glazing types, at maximum heat carrier heating, the efficient factor and amount of incoming solar radiation heat to the collector with double glazing is more perfect, than with a single layer glazing. It proves, that we have selected proper solar collector's parameters and the collector operates in the normal mode in any weather conditions.

REFERENCES

1. *Weiss, W., Spörk-Dür, M., Mauthner, F., Solar Heat Worldwide Global Market Development and Trends in 2016. Shc 86., 2017.*
2. *N.S. Suresh, B.S. Rao. Solar energy for process heating: a case study of select Indian industries. J. Clean. Prod., 151 (2017), pp. 439-451, 10.1016/J.JCLEPRO.2017.02.190.*
3. *A. Hassanzadeh, Experimental Study on Increasing the Electrical Efficiency of Photovoltaic Panel with Decreasing Rear Surface Temperature, Sharif University of Technology, 2015.*
4. *M. Abdelhamid, B.K. Widyolar, L. Jiang, R. Winston, E. Yablonovitch, G. Scranton, D.*
5. *Cygan, H. Abbasi, A. Kozlov. Novel double-stage high-concentrated solar hybrid photovoltaic/thermal (PV/T) collector with nonimaging optics and GaAs solar cells reflector.Appl. Energy (2016), 10.1016/j.apenergy.2016.07.127.*
6. *H.E.S. Fath, S.M. Elsherbiny, A.A. Hassan, M. Rommel, M. Wieghaus, J. Koschikowski, M.Vatansever. PV and thermally driven small-scale, stand-alone solar desalination systems with very low maintenance needs. Desalination, 225 (2008), pp. 58-69, 10.1016/J.DESAL.2006.11.029.*
7. *R. Shukla, K. Sumathy, P. Erickson, J. Gong, Recent advances in the solar water heating systems: a review. Renew. Sustain Energy Rev. (2013), 10.1016/j.rser.2012.10.048.*
8. *H. Guo, H.M. Ali, A. Hassanzadeh, Simulation study of flat-sheet air gap membrane distillation modules coupled with an evaporative crystallizer for zero liquid discharge water desalination Appl. Therm. Eng., 108 (2016), pp. 486-501, 10.1016/j.applthermaleng.2016.07.131.*
9. *Tian, J. L., Zhang, H. Y., Wang, G. G., Wang, X. Z., Sun, R., Jin, L., & Han, J. C. (2015). Influence of film thickness and annealing temperature on the structural and optical properties of ZnO thin films on Si (1 0 0) substrates grown by atomic layer deposition. Superlattices and Microstructures, 83, 719-729.*
10. *P.D. Jose, The flux through the focal spot of a solar furnace. Sol. Energy, 1 (4) (1957), pp. 19-22.*
11. *D.L. Evans. On the performance of cylindrical parabolic solar concentrators with flat absorbers. Sol. Energy, 19 (1977), pp. 379-385.*
12. *J.C. Daly. Solar concentrator flux distributions using backward ray tracing. Appl. Opt., 18 (1979), pp. 2696-2700*
13. *R.O. Nicolas. Optical analysis of cylindrical-parabolic concentrators: validity limits for models of solar disk intensity. Appl. Opt., 26 (18) (1987), pp. 3866-3870*
14. *S.M. Jeter, Analytical determination of the optical performance of practical parabolic trough collectors from design data. Sol. Energy, 39 (1) (1987), pp. 11-21.*
15. *N.D. Kaushika. Viability aspects of paraboloidal dish solar collector systems. Renew. Energy, 3 (1993).*
16. *Kalogirou, S., 1996. Artificial neural network for predicting the local concentration ratio of parabolic trough collectors. In: International Proceedings Eurosun'96, Freinberg (Germany), pp. 470–475.*
17. *Gombert, W. Glaubitt, K. Rose, J. Dreibholz, B. Blasi, A. Heinzel, D. Sporn, W. Doll, V.Wittwer. Antireflective transparent covers for solar devices. Sol. Energy, 68 (4) (2000), pp. 357-360.*
18. *M. Eck, W.D. Steinmann. Modelling and design of direct solar steam generating collector fields. J. Sol. Energy Eng. Trans. ASME, 127 (2005), pp. 371-380.*

19. *Bhattacharya, A. (2018). Why is Nigeria Adichie's Lowland? A Comparative Study of Jhumpa Lahiri's the Lowland and Chimamanda Adichie's Half of a Yellow Sun.*
20. *R. Grena. Optical simulation of a parabolic solar trough collector. Int. J. Sustain. Energy, 29 (2010), pp. 19-36.*
21. *Yang, B., Zhao, J., Xu, T., Zhu, Q., 2010. Calculation of the concentrated flux density distribution in parabolic trough solar concentrators by Monte Carlo ray-trace method. 2010 Symp. Photonics and Optoelectron., Chengdu, 2010.*
22. *Kumar, K.R., Reddy, K.S., 2010. Determination of concentrated flux intensity distribution for solar parabolic trough concentrator. In: Proceedings of 9th International Conference on Sustainable Energy Technologies, Shanghai, China, 24–27 August 2010, pp. 205.*
23. *Khandekar, D. B., Vanjari, A., & Patil, R. A. Design of the Electric antenna for the detection of the coronal Mass Ejections from the sun. In 2014 International Conference on Signal Propagation and Computer Technology (ICSPCT 2014).*
24. *Y.L. He, J. Xiao, Z.D. Cheng, Y.B. Tao. A MCRT and FVM coupled simulation method for energy conversion process in parabolic trough solar collector. Renew. Energy, 36 (2011), pp. 976-985.*
25. *T. Cooper, A. Steinfeld. Derivation of the angular dispersion error distribution of mirror surfaces for Monte Carlo ray-tracing applications. J. Sol. Energy Eng., 133 (2011), p. 044501.*
26. *F. Francini, D. Fontani, P. Sansoni, L. Mercatelli, D. Jafrancesco, E. Sani. Evaluation of surface slope irregularity in linear parabolic solar collectors. Int. J. Photoenergy, 2012 (2012).*
27. *M. Wirz, M. Roesle, A. Steinfeld. Three-dimensional optical and thermal numerical model of solar tubular receivers in parabolic trough concentrators. J. Sol. Energy Eng., 134 (2012), pp. 1-9.*
28. *Z.D. Cheng, Y.L. He, F.Q. Cui, B.C. Du, Z.J. Zheng, Y. Xu. Comparative and sensitive analysis for parabolic trough solar collectors with a detailed Monte Carlo ray-tracing optical model. Appl. Energy, 115 (2014), pp. 559-572.*
29. *Hameed, A. A., Al-Fatlawy, N. M., & Al-Salehi, A. M. (2017). Estimation of hourly global solar radiation incident of inclined surface in Iraq at different sky condition. Int. J. Res. Appl. Nat. Soc. Sci, 5, 13-28.*
30. *Amirgaliyev, Y.N., Kunelbayev, M., Wójcik, W., Kozbakova, A.K., Irzhanova, A.A.Solar-driven resources of the Republic of Kazakhstan.News of the National Academy of Sciences of the Republic of Kazakhstan, Series of Geology and Technical Sciences.2018,3(430),pp 18-27.*
31. *Nina G. Jablonski and George Chaplin. Human skin pigmentation as an adaptation to UV radiation. Proc Natl Acad Sci U S A. 2010 May 11; 107(Suppl 2): 8962–8968.*
32. *Kultan J., Baitassov T., Ishankulov M., Rivkina N. Climatic conditions of Astana For the development of alternative energy sources. 4 International Conference Renewable Energy Sources. May 21-23, 2013 Tatranské Matliare. Slovak Republic.*
33. *Evangelos Bellos and Christos Tzivanidis. Analytical Expression of Parabolic Trough Solar Collector Performance. Designs 2018, 2, 9, pp 1-17.*
34. *Chung-Yu Tsai. Optimized solar thermal concentrator system based on free-form trough reflector. Solar Energy, 125, 2016, pp 146-160.*